

# Comparative study of size dependent four-point probe sheet resistance measurement on laser annealed ultra-shallow junctions

Dirch Hjorth Petersen<sup>a)</sup>

*MIC—Department of Micro and Nanotechnology, Nano-DTU, Technical University of Denmark (DTU), Building 345 East, DK-2800 Kongens Lyngby, Denmark and Capres A/S, Scion-DTU, Building 373, DK-2800 Kongens Lyngby, Denmark*

Rong Lin

*Capres A/S, Scion-DTU, Building 373, DK-2800 Kongens Lyngby, Denmark*

Torben Mikael Hansen

*MIC—Department of Micro and Nanotechnology, Nano-DTU, Technical University of Denmark (DTU), Building 345 East, DK-2800 Kongens Lyngby, Denmark and Capres A/S, Scion-DTU, Building 373, DK-2800 Kongens Lyngby, Denmark*

Erik Rosseel

*IMEC, Kapeldreef 75, B-3001 Leuven, Belgium*

Wilfried Vandervorst

*IMEC, Kapeldreef 75, B-3001 Leuven, Belgium and K.U. Leuven, Electrical Engineering Department, INSYS, Kasteelpark Arenberg 10, B-3001 Leuven, Belgium*

Christian Markvardsen, Daniel Kjær, and Peter Folmer Nielsen

*Capres A/S, Scion-DTU, Building 373, DK-2800 Kongens Lyngby, Denmark*

(Received 31 May 2007; accepted 14 September 2007; published 31 January 2008)

In this comparative study, the authors demonstrate the relationship/correlation between macroscopic and microscopic four-point sheet resistance measurements on laser annealed ultra-shallow junctions (USJs). Microfabricated cantilever four-point probes with probe pitch ranging from 1.5 to 500  $\mu\text{m}$  have been used to characterize the sheet resistance uniformity of millisecond laser annealed USJs. They verify, both experimentally and theoretically, that the probe pitch of a four-point probe can strongly affect the measured sheet resistance. Such effect arises from the sensitivity (or “spot size”) of an in-line four-point probe. Their study shows the benefit of the spatial resolution of the micro four-point probe technique to characterize stitching effects resulting from the laser annealing process. © 2008 American Vacuum Society. [DOI: 10.1116/1.2794743]

## I. INTRODUCTION

Maintaining adequate device performance within the continued miniaturization of semiconductor devices necessitates the development of extremely shallow (<20 nm) source/drain extensions with very high dopant concentration and electrical activation level.<sup>1</sup> As the millisecond annealing process used for ultra-shallow junction (USJ) formation today only leads to partial (metastable) activation, one can no longer assume 100% activation. Thus, the dopant profile is no longer a good measure for the electrically active carrier profile, and secondary ion mass spectroscopy profiles cannot accurately predict the sheet resistance, which is of utmost importance. Sheet resistance measured with conventional four-point probes has for many decades been used to characterize the doped region. However, conventional four-point probe measurements are seriously hampered by probe penetration, leading to excessive sampling of the underlying substrate.<sup>2</sup> Hence, alternative approaches for characterization of sheet resistance are presently being investigated based on optical tools, noncontact measurements, or four-point probe

systems with drastically reduced probe penetration. The micro four-point probe (M4PP) technology developed at MIC (Ref. 3) and Capres A/S (Ref. 4) has proved to be a possible candidate to measure the sheet resistance of USJ as it provides an evaluation of the sheet resistance without the artifacts of probe penetration. Moreover, its drastically reduced electrode separation enables the analysis of sheet resistance variations on a much finer scale than feasible previously.

In this work, the M4PP was used to probe the lateral sheet resistance uniformity of laser annealed junctions. Periodic features related to the stitching overlays of the laser beams as well as nonuniformities within the laser beam itself can be clearly resolved. Using probes with various dimensions, the probe pitch effects on these measurements could be clearly resolved. A theoretical interpretation of its smoothing effect and the role of the actual measurement configuration are presented.

## II. EXPERIMENT

In this study, an ultra-shallow junction was formed by low energy <sup>11</sup>B implantation (0.5 keV and  $1 \times 15 \text{ cm}^{-2}$ ) into a lowly doped 300 mm *n*-type Si wafer followed by laser an-

<sup>a)</sup>Electronic mail: dhp@mic.dtu.dk

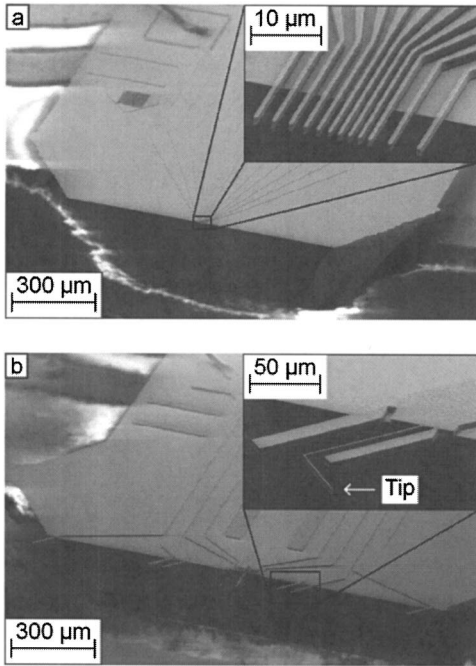


FIG. 1. Scanning electron micrographs of (a) a multicantilever probe with minimum electrode pitch of  $1.5 \mu\text{m}$  and (b) a  $500 \mu\text{m}$  pitch four-point probe with L-shaped static contact cantilevers.

nealing. The laser anneal aimed at a nominal anneal temperature of  $1300^\circ\text{C}$ , resulting in a junction depth of  $20 \text{ nm}$  at  $1 \times 18 \text{ cm}^{-3}$ . The laser beam was scanned in straight lines across the sample surface with a step size of  $3.65 \text{ mm}$ , whereas its spot size is significantly larger ( $\sim 11 \text{ mm}$ ) such that the scanned lines overlap and each region is irradiated several times.

To avoid a contribution from probe penetration, conventional four-point probes were not used for comparison in this work and all results were obtained with M4PP (Capres) and similar cantilever four-point probes. These four-point probes consist of micromachined cantilever electrodes extending from the edge of a silicon support. The cantilevers consist of silicon oxide or silicon coated with a metal thin film and provide extremely low contact forces ( $\sim 10^{-5} \text{ N}$ ).<sup>3</sup> Probes were fabricated with an electrode pitch ranging from  $1.5$  to  $500 \mu\text{m}$  (cf. Fig. 1) and their specifications are summarized in Table I.

For the large pitch four-point probes ( $\geq 50 \mu\text{m}$ ), the alignment between probe and sample is critical as all four cantilevers should contact the surface at the same time. Any

TABLE I. Specifications of four-point probes used in this work.

Electrode pitch ( $\mu\text{m}$ )	Cantilever material	Electrode material	Cantilever geometry	Spring constant (N/m)
1.5	$\text{SiO}_2$	Ti/Ni	Straight beam	$\sim 20$
7–20	Polysilicon	Ti/Ni or Ti/Au	Straight beam	$\sim 50$
50–500	Polysilicon	Ti/Ni or Ti/Au	L shaped	$\sim 1-10$

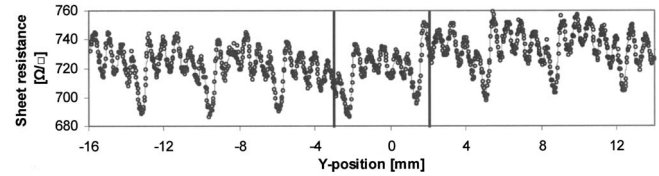


FIG. 2. 30 mm sheet resistance line scan perpendicular to the laser scan direction using a  $10 \mu\text{m}$  pitch four-point probe and a step size of  $25 \mu\text{m}$ . The vertical lines define the area which was consecutively probed with different probe pitches (cf. Fig. 3). A continuous function of the sheet resistance was approximated (thin line) for finite element method (FEM) simulations (cf. Fig. 9).

misalignment will necessitate the use of excessive contact force which could possibly result in surface scratching and extreme probe wear. For this reason static contact cantilevers were designed with an L-shaped high aspect ratio geometry to eliminate/minimize surface movements.<sup>5</sup>

The choice of Ni or Au as electrode material does not impact the measurement precision but can affect probe lifetime/wear and of course acceptability in a complementary metal-oxide semiconductor–production environment. All the scans presented in this work have been measured in a random mode (meaning that the sheet resistance data are measured in random order) to rule out any periodic variations in the measurement condition, and no deterioration of the sheet resistance precision over the probe life span has been observed. The four-point measurements were performed with the four electrodes being placed on a line orthogonal to the laser annealing scan direction and in a dual configuration mode based on the A and C configurations [cf. Fig. 7 and Eq. (2)].

### III. UNIFORMITY OF LASER ANNEALING

To study the (local) inhomogeneities following laser annealing, a 30 mm line scan was measured with a  $10 \mu\text{m}$  pitch M4PP and a step size of  $25 \mu\text{m}$  in a direction perpendicular to the laser scan direction. The result is shown in Fig. 2 and indicates significant periodic sheet resistance variations.

In order to study the periodic variations in more detail and the impact of electrode pitch on these results, a 5 mm line scan was measured repeatedly with 11 different electrode pitches. All these measurements were performed in the same region, as indicated by the vertical lines in Fig. 2.

In Fig. 3, we selectively plot six characteristic 5 mm long line scans obtained using different electrode pitches. The measurement results demonstrate the electrode pitch effect on the measured sheet resistance. The largest probe pitch ( $500 \mu\text{m}$ ) significantly smoothens out the resistance values and “characterizes” the sheet resistance as being more homogeneous than the smaller pitch probes ( $\leq 20 \mu\text{m}$ ).

To quantify the smoothening effect of the large pitched probes, the relative standard deviation and peak-to-peak variation of the sheet resistance are calculated and plotted as a function of probe pitch in Fig. 4. In these plots, we restrict the calculations to the oscillations within one period (i.e.,

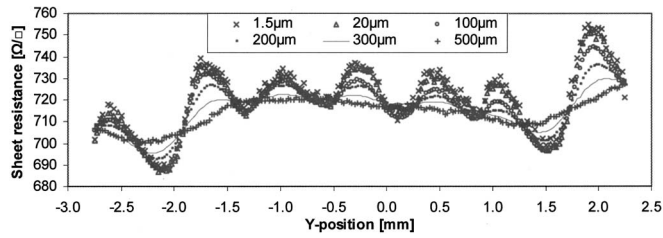


FIG. 3. Raw data of a 5 mm line scan with 25  $\mu\text{m}$  step size repeated at the same location with various pitched four-point probes to compare macro and micro sheet resistances. Only selected electrode pitch results are shown for easy comparison.

3.65 mm and 750  $\mu\text{m}$  for the two main periods observed in Fig. 2—the corresponding line segments are illustrated in Fig. 5). It is clear that the sheet resistance standard deviation and peak-to-peak variation obtained with the large pitched four-point probes are much less than those obtained using M4PP with 1.5–20  $\mu\text{m}$  pitch for both periods. A small increase in sheet resistance variation is seen with the 500  $\mu\text{m}$  pitch probe relative to the 300–450  $\mu\text{m}$  pitch probes for the 750  $\mu\text{m}$  period [cf. Fig. 4(b)]. However, this is likely an artifact caused by other variations such as the 3.65 mm period, i.e., the 500  $\mu\text{m}$  pitch probe is larger than the line scan itself.

Figure 5 illustrates the two line segments used for the calculations of the sheet resistance variation. The vertical

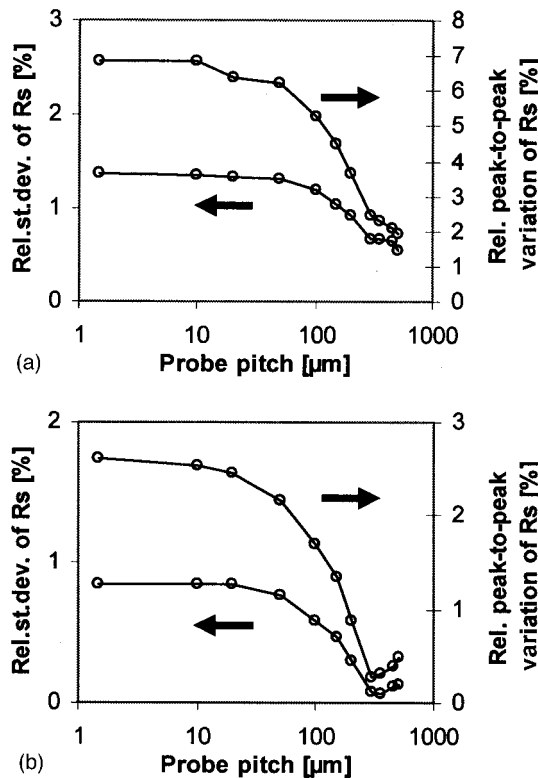


FIG. 4. Comparison of the relative standard deviation and relative peak-to-peak variation of the sheet resistance measured with different electrode pitches for (a)  $Y = (-1.825, 1.825)$  mm [cf. Fig. 5(a)] and (b)  $Y = (0.10, 0.85)$  mm [cf. Fig. 5(b)].

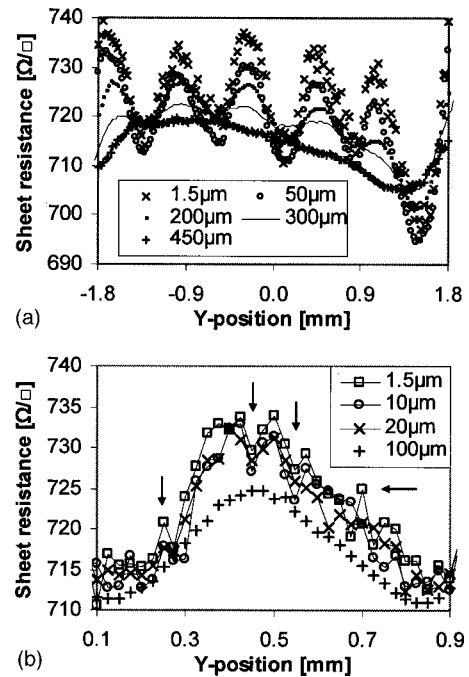


FIG. 5. Selected electrode pitch and line segment of the 5 mm line scan in Fig. 3. A line segment was chosen to represent the two main periodic variations of (a) 3.65 mm and (b)  $\sim 750$   $\mu\text{m}$ .

arrows [on Fig. 5(b)] point to unexpected coincident sheet resistance peaks and valleys obtained with the small pitched probes ( $\leq 20$   $\mu\text{m}$ ). The horizontal arrow on the same figure points to a resistance peak obtained with the 1.5  $\mu\text{m}$  pitch probe. This peak is not resolved by the 10 and the 20  $\mu\text{m}$  pitch probe, and it remains to be proved if these variations are true or accidental measurement error.

In order to probe nonhomogeneities in the laser scan direction, a full two dimensional (2D) map was made using a 10  $\mu\text{m}$  pitch M4PP and scan step sizes of 50 and 250  $\mu\text{m}$  in the  $X$  and  $Y$  directions, respectively. The result shown in Fig. 6 indicates not only the periodic pattern in the  $Y$  direction but

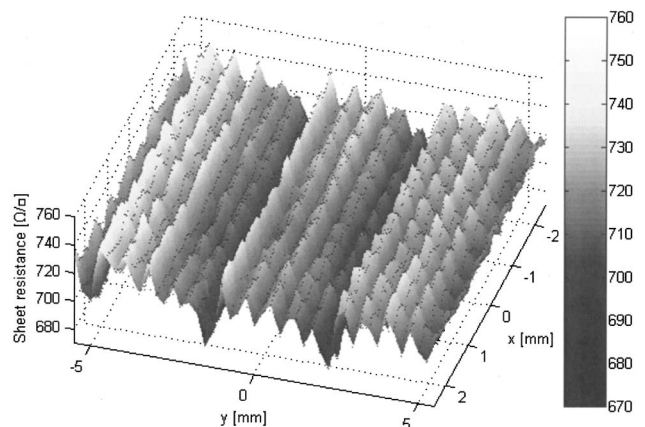


FIG. 6.  $45 \times 101$  point area scan measured with a 10  $\mu\text{m}$  pitch M4PP. The scan step sizes are 50 and 250  $\mu\text{m}$  in the  $X$  and  $Y$  directions, respectively. Raw data are represented by dots.

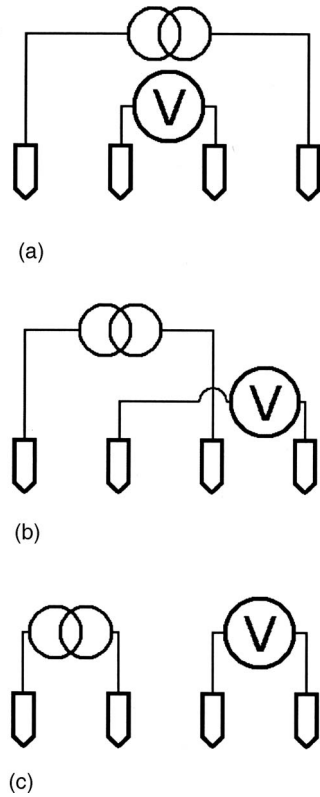


FIG. 7. Illustration of three independent four-point configurations, (a) A, (b) B and (c) C configurations.

also an apparent sheet resistance variation in the  $X$  direction with a period of roughly  $500 \mu\text{m}$ . The peak-to-peak variation in the  $X$  direction is roughly  $30 \Omega/\square$  (or 4%). The cause of these variations could be time dependent fluctuations in temperature, laser movement, laser power, etc., and is the subject of further investigation.

#### IV. DISCUSSION

Prior to the discussion of the origin of the electrode pitch effect, it is important to address the issue of the probe configuration itself. Basically, there exist three independent probe configurations (Fig. 7) for an in-line four-point probe which can be used to extract the sheet resistance of a conductive infinite sheet.

Generally, the sheet resistance  $R_S$  is calculated from<sup>6</sup>

$$R_S = \frac{V}{I}c, \quad (1)$$

where  $I$  is the applied current,  $V$  is the measured voltage, and  $c$  is a geometrical correction factor that depends on the sample shape and the contact positions. The in-line four-point measurement can be shown to be a special case of a van der Pauw measurement,<sup>7</sup> and Rymaszew has used the ideas of van der Pauw to perform position correction valid for an infinite sheet.<sup>8</sup> In the dual configuration mode, the resistance is measured in two of the independent probe configurations, e.g., A and C, and the sheet resistance is calculated based on these two measurements,

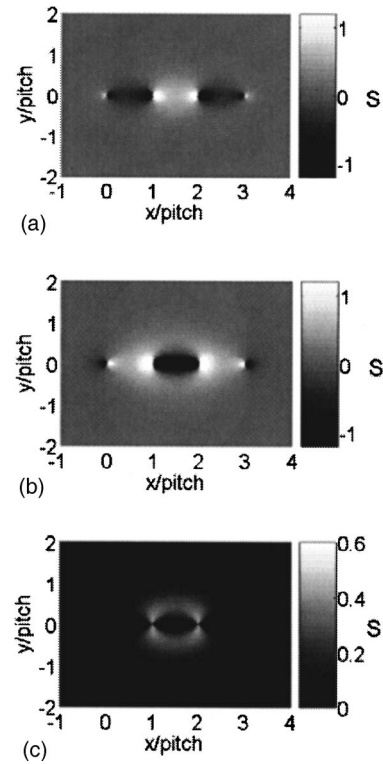


FIG. 8. Contour plots of the sensitivity to resistance variations for an in-line four-point probe in the A, C, and dual configuration modes, (a), (b), and (c), respectively. The four contacts are positioned at  $(x, y) = (0, 0)$ ,  $(1, 0)$ ,  $(2, 0)$ , and  $(3, 0)$ . The sensitivity goes to  $\pm$ infinity at the contact points for the A and C configurations; however, the color scale has been cut off (at  $S = \pm 1.2$ ) to see the surrounding contour. The color scale has not been cut off for the dual configuration contour plot.

$$\exp\left(\frac{-2\pi R_A}{R_S}\right) + \exp\left(\frac{-2\pi R_C}{R_S}\right) = 1, \quad (2)$$

where  $R_A$  and  $R_C$  are the four-point voltage-to-current ratios measured with the A and C configurations, respectively. If the contact points are located along a straight line, positional error along the line is eliminated<sup>8,9</sup> and off-line positional errors influence the measurement only as a second order effect.<sup>9</sup> If the infinite sheet has an otherwise homogeneous sheet resistance, the sensitivity  $S$  to local resistance variations  $R_{S,L}$  may be calculated using the adjoint system method<sup>10,11</sup> adapted to the dual configuration mode.<sup>9</sup> The normalized four-point probe sensitivity is defined as

$$S = \frac{\partial^2 R_S}{\partial R_{S,L} \partial A} p^2, \quad (3)$$

where  $A$  is the area and  $p$  is the electrode pitch. To get the change in measured sheet resistance, the sensitivity must be integrated over the affected area; e.g., when measuring with an electrode pitch of  $500 \mu\text{m}$  if an area of  $50 \times 50 \mu\text{m}^2$  with a constant sensitivity of 1 changes by  $100 \Omega/\square$ , then the measured sheet resistance will change by only  $1 \Omega/\square$ . It follows that a smaller probe pitch must be used to correctly characterize such an area.

In Fig. 8, the sensitivity  $S$ , as defined by Eq. (3), is plotted



for an equidistant electrode pitch. Shown are sensitivities for A, C, and dual configuration modes. Configuration B shows a similar sensitivity characteristic as configuration A. For the correct interpretation of the following results, it is important to notice that an in-line four-point probe measuring in the A and C configurations has an opposite sign of sensitivity to sheet resistance variations. This means that if a thin film with otherwise homogeneous sheet resistance has an increased resistance at some point, the sheet resistance measured with a four-point probe centered at this point will be higher for the A configuration and lower for the C configuration. Negative sensitivity has previously been reported by Koon and Knick-erbocker for the A configuration and dual configuration.<sup>12</sup> They do not find the negative sensitivity to be eliminated as in the case of the dual mode applied here. However, this may be due to an error in normalization of the sensitivity.<sup>13</sup>

In order to verify the experimental results of the electrode pitch size effect, theoretical simulations using a finite element method (FEM) were performed. In these simulations, we used a two dimensional sheet with a spatial variation in sheet resistance based on the 30 mm line scan of Fig. 2 (the sheet resistance is defined by an approximated continuous (wave) function of  $Y$  and with no variation in the  $X$  direction). The FEM simulations were performed with COMSOL 3.3 using a 2D model (Conductive Media DC). An electrode pitch of  $500\ \mu\text{m}$  was used, and it was verified that the simulations were insensitive to further mesh refinements and did not suffer from edge effects.

The results are compared in Fig. 9 to the assumed sheet resistance variation and the experimental data for the corresponding electrode pitch. Whereas the pattern can clearly reproduce, the absolute differ slightly, probably due to the approximations used to describe the sample. It is also interesting to see the impact of the measurement mode. For instance, it appears that the A configuration gives the most “correct” sheet resistance variation, whereas the C configuration gives a completely out-of-phase sheet resistance pattern, turning peaks into valleys. The apparent good result of the A configuration mode is due to an interferencelike behavior of the positive and negative sensitivities for single configuration measurements. If the sheet resistance was not periodic but rather spikelike (only half-period on an otherwise homogeneous sample), the A configuration would not give a trustworthy representation of the sheet resistance.<sup>14</sup> For the same reason the dual configuration  $500\ \mu\text{m}$  pitch probe smoothens the sheet resistance because it only has positive sensitivity. In either case, the conclusion is clear that the  $500\ \mu\text{m}$  pitch probe leads to unreliable results and cannot be used to assess these small scale variations.

## V. CONCLUSION

Accurate sheet resistance characterization of ultra-shallow implants is crucial for further development of CMOS transistors. From this study, it is evident that due to their smaller sampling volume, micro four-point probes can resolve sheet resistance variations more precisely than conventional sized four-point probes.

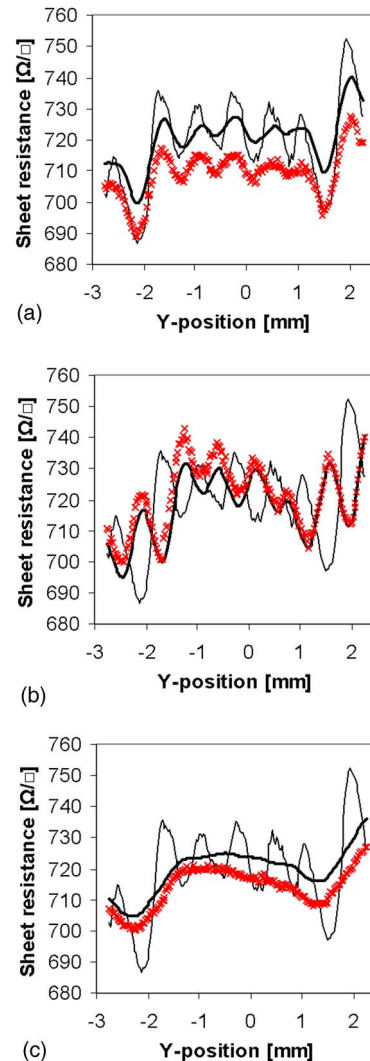


FIG. 9. Comparison of A, C, and dual configurations, (a), (b), and (c), respectively, for a  $500\ \mu\text{m}$  pitch four-point probe on a nonhomogeneous USJ. The thin line represents the surface sheet resistance as defined for the FEM simulations (which corresponds to the sheet resistance measured with a  $10\ \mu\text{m}$  pitch M4PP). The thick line is the FEM simulated result and the cross represents the experimentally measured result (raw data).

This is illustrated in detail by analyzing the (local) non-uniformities of laser annealed junctions. Periodic patterns related to the laser scan overlay pattern and laser beam non-uniformities are observed. These can be characterized in much more detail when using a fine electrode pitch, whereas the regular  $500\ \mu\text{m}$  pitch leads to an excessive smoothing, thereby obscuring the finer details of the laser anneal process.

A theoretical analysis of the four-point measurements has been performed, assessing the sensitivity of the various configuration modes to small local sheet resistance variations. Whereas in a dual configuration mode, the sensitivity is purely positive, a single configuration four-point measurement may exhibit both positive and negative sensitivities to resistance variations leading to an unexpected correlation to local inhomogeneities. Based on this formalism also, the ef-

fect of electrode pitch on the measurements has been simulated. These simulations confirm the experimental observations that the 500  $\mu\text{m}$  pitch four-point probe significantly underestimates the sheet resistance variations present on a laser annealed ultra-shallow junction (20 nm).

## ACKNOWLEDGMENTS

The authors are grateful for the financial support from Copenhagen Graduate School for Nanoscience and Nanotechnology (C:O:N:T) and the Danish Research Agency (FTP), and acknowledge valuable discussions with Ole Hansen and Peter Bøggild.

<sup>1</sup>International Technology Roadmap for Semiconductors (ITRS), Front End Processes (<http://www.itrs.net>).

<sup>2</sup>T. Clarysse *et al.*, *MRS Spring Meeting, San Francisco, US, 2006* (Materials Research Society, Warrendale, 2006), p. 197.

rials Research Society, Warrendale, 2006), p. 197.

<sup>3</sup>C. L. Petersen, T. M. Hansen, P. Boggild, A. Boisen, O. Hansen, T. Hassenkam, and F. Grey, *Sens. Actuators, A* **96**, 53 (2002).

<sup>4</sup><http://www.capres.com>

<sup>5</sup>D. H. Petersen, O. Hansen, T. M. Hansen, P. R. E. Petersen, and P. Boggild, 33rd International Conference on Micro- and Nano-Engineering 2007, Copenhagen, Denmark, p. 409.

<sup>6</sup>F. M. Smits, *Bell Syst. Tech. J.* **37**, 711 (1958).

<sup>7</sup>L. J. van der Pauw, *Philips Res. Rep.* **13**, 1 (1958).

<sup>8</sup>R. Rymaszew, *J. Phys. E: J. Sci. Instrum.* **2**, 170 (1969).

<sup>9</sup>T. M. Hansen, D. H. Petersen, R. Lin, D. Kjær, and P. F. Nilsen (unpublished).

<sup>10</sup>L. K. J. Vandamme and W. M. G. van Bokhoven, *Appl. Phys.* **14**, 205 (1977).

<sup>11</sup>L. K. J. Vandamme and G. Leroy, *Fluct. Noise Lett.* **6**, L161 (2006).

<sup>12</sup>D. W. Koon and C. J. Knickerbocker, *Rev. Sci. Instrum.* **63**, 207 (1992).

<sup>13</sup>D. W. Koon (private communication).

<sup>14</sup>T. M. Hansen, K. Stokbro, O. Hansen, T. Hassenkam, I. Shiraki, S. Hasegawa, and P. Boggild, *Rev. Sci. Instrum.* **74**, 3701 (2003).